ICSP2008 Proceedings

Detection of coded concentric rings for camera calibration

Jing Chen，Lihui Wang, Baozong Yuan
Institute of Information Science, Beijing Jiaotong University, Beijing 100044, P. R. China
E-mail：03112026@bjtu.edu.cn

Abstract

A fast and accurate coded marker identification method is presented in this paper. The method combines image processing techniques with prior information of marker's appearance and shape. The deformation of the circle caused by projection is considered so that the marker can be recognized correctly. The experiments demonstrate the robustness and accuracy of our method.

1. Introduction

Feature points detection and matching are very important for camera calibration in computer vision and photogrammetry. Although many natural feature points, such as corners, edges, affine invariant regions etc, can be detected and matched correctly among images taken from different views, they are not always stable and accurate. So artificial markers (see Fig. 1) have been designed for the purpose of automatic matching.

The markers in Fig. 1 have many distinctive features. The regular shapes such as circle and rectangle, homogenous texture on appearance make them very easy to be detected. The coding information embedded in the form of circular dot (see Fig. 1(a)), section angle (see Fig. 1(b) and (c)), ring color (see Fig. 1(d)) and two dimension bar code (see Fig. 1(e)) gives exclusive matching results. So the artificial markers are widely used in augmented reality, automatic 3D-measurement and camera calibration.

In this paper, we intend to describe a system for one kind of marker identification and its application to camera calibration. Our system can attack high dynamic range of light and large deformation caused by projection.

2. Geometric design of marker

Figure 2 (a) shows an example of the marker. It has an outer data ring and an inner white ring with a black "eye" in the center. As shown in figure 2 (b), the data ring is divided into 12 sectors evenly and each sector occupies 30 degrees and represents 0 or 1 by filling white or black color. The marker can be represented by a code of 12 bits (see Fig. 2 (c)). There are 2^{12} markers corresponding to 12 sectors in theory. But ring is invariant to rotation. That means the different codes which are generated by assigning different starting sector in the same marker are equal. Derived from Burnside's theorem, there are 352 different markers totally.

The radius of the outer circle on the border of the data ring is r_2 . The radius of the "eye" which is designed for marker location is r_1. We keep the ratio r_{21} of r_2 to r_1 fixed when we print the markers. The white space left between r_2 and r_1 is to prevent data ring and "eye" from aliasing during image formation.

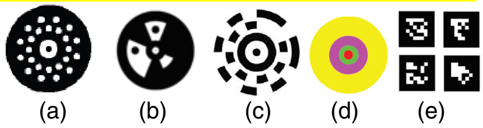

Figure 1. Artificial Markers

3. Previous work

TRIP[1] (see Fig. 1 (c)) is a vision-based marker location system for ubiquitous computing. It binarizes the image by adaptive thresholding and detects the concentric circle ring codes by ellipse fitting.

Naimark and Foxlin[2] (see Fig. 1 (b)) implement a modified homomorphic image processing technique to handle the problem of light varying. They locate the candidate marker by selecting the white elliptical region and read the code from local coordinate defined by three eyes.

Cho and Neumann[3] (see Fig. 1 (d)) employ multi-scale concentric color ring to increase the camera operating range. The center of the ring is computed from the edge points and the code is embedded in the different colors.

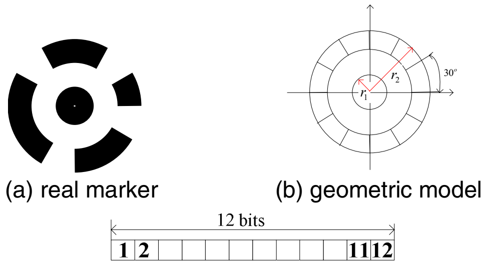

Figure 2. Coded concentric ring

Ahn and Rauh[4] (see Fig. 1 (a)) present a circular coded target for automatic image point measurement and identification. They recognize the target by the arrangement of the dots around the central concentric ring. Ellipse fitting plays an important role through all of the processing stages.

Claus and Fitzgibbon[5] identify the change of lighting, scale and foreshortening as major obstacles to viosion-based marker detection. Their schematic adapts to natural scenes within a machine learning framework.

ARTag[6] (see Fig. 1 (e)) is a marker system that uses digital coding theory to get a low false positive and inter-marker confusion rate with a small marker size, employing an edge linking method to give robust lighting variation immunity.

These existing systems identify their markers by exploiting marker features as much as possible. Our system is inspired by some of them.

4. Image processing for finding the marker

The marker described in section 2 is used by PhotoModeler™[7], AICON™[8] and 3DM-FotoMetrics[9]. But the mechanism how they work is unknown. In this paper, we present a system which can handle detection and recognition of this kind of marker fast and accurately. The architecture is shown in Figure 3. It consists of two parts, detection and recognition. Detection which includes six blocks aims to find the elliptical region that the central "eye" of the marker may reside in. Recognition which has three blocks decodes the data ring. We will introduce each block in the following sections.

4.1. Marker detection

It is well known that the gray value of the pixel varies tremendously according to different illumination, for example, white paper can change from 70 to 255 in 8-bit gray scale values, while black is typically 20-50[2]. This phenomenon does much harm to find the black blob by thresholding. Jae in his book[10] introduces a concept of homomorphic processing to weaken this value fluctuation. Homomorphic processin

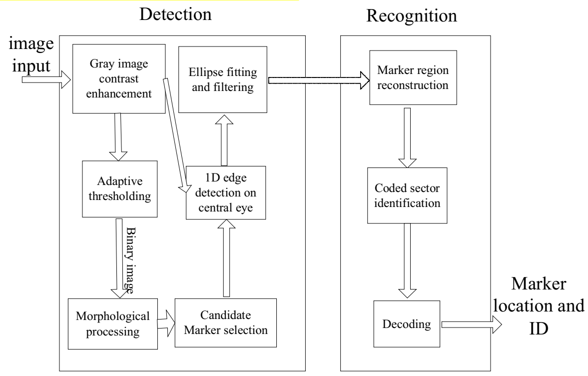

Figure 3. Marker identification architecture

-g is to model the grayscale image as a product of illumination and reflectance values:

$f(u,v)=i(u,v)\times r(u,v)$ (1)

and assumes that the illumination factor $i(u,v)$ varies relatively slowly compared to the reflectance $r(u,v)$.

In order to separate i and r into additive terms, logarithm of the image is taken as

$\log f(u,v)=\log i(u,v)+\log r(u,v)$ (2),

then apply a high-pass filter designed to attenuate the slowly-varying illumination term. We need not exponentiate the filtered image to a good looking one because our goal is to threshold the image.

Following homomorphic processing, we apply an adaptive thresholding method[11], which chooses the threshold to minimize the intraclass variance of the black and white pixels, to transform the gray image to binary image. There may be many small black dots whose size is much smaller than our object of the marker's "eye" in the binary image. We eliminate them by performing morphological opening operation. Disk is chosen as the structuring element.

After morphological opening, connected components labeling is carried out. It groups the binary-0 pixels into maximal connected regions. All pixels that have value binary-0 and are connected to each other by a path of pixels all with value binary-0 are given the same identifying label. The efficient union-find algorithm[12] is used here. At the same time, the properties (center, area, shape) of the labeled region are computed. We are only concerned with regions corresponding to the perspective projections of the balck "eye" of the marker, i.e. ellipses. So we take two tests on the regions for finding them:

1. Area approximation test: Since eyes are circles, they must appear approximately elliptical in images, which implies $A \approx \pi r_{maj} r_{min}$, where A is the region area, r_{maj} and r_{min} are the semi-axis. All of them can be computed from region moments.

2. Shape similarity test: the ratio of r_{maj} to r_{min} must not be too much. This test can filter out narrow objects.

Typically after all weed-out tests we have 90% of the good marker "eyes" plus a few extraneous objects selected as candidates for decoding.

Although the ellipse parameters can be estimated from region moments, the accuracy is not high enough to transform the deformed marker back to original shape for decoding. So we compute the exact parameters by fitting of the edge points. It is not necessary to implement edge detection on the whole image. We only detect two jump points along the ray, shown in Figure 4 (a), from the candidate region center in the contrast enhanced image. The ray is convoluted with a derivative of 1D Gaussian kernel. Its edge points are the local extrema (Fig. 4 (b)) of the convoluted signal. The ray is rotated evenly around the center and the edge is sampled. Then the direct least-squares ellipse fitting method developed by Pilu et al.[13] is applied to all edge points. Thanks to the accurate 1D edge detection, the fitting error can be a criterion for candidate marker selection.

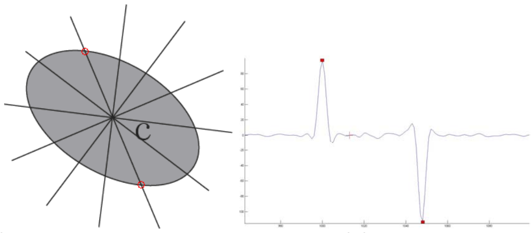

(a) "Rays" emanating from center (b) Edge points

Figure 4. 1D edge detection on ray

4.2. Marker Recognition

After obtaining the ellipse parameters that best approximate the 1D edge points, the code deciphering stage is undertaken. We return to the binary image and compute the marker region according to the known ellipse's semi-axis and the ratio r_{21} . After some simple but tedious manipulations of cross ratio, the region that the projected marker occupies can be approximated by enlarging the its central ellipse r_{21} times. we may obtain the reconstructed marker (Fig. 5 (b)) by rotating, scaling the deformed one (Fig. 5 (a)) according to the five ellipse parameters of the "eye".

A valid coding sector must find itself in a ring shaped zone around the circle black "eye", and reversibly, a valid "eye" must have a valid arrangement of the coding sector around it. The above is another crit

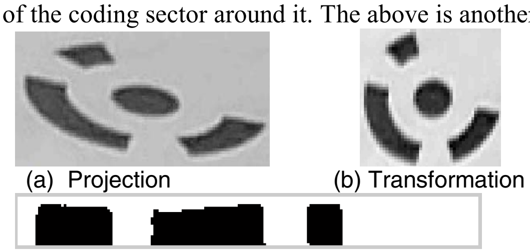

(a) Projection (b) Transformation

(c) Rectification

Figure 5. Marker recognition

-erion for marker selection. Computing the angle of the black circular sector directly is not effective. The polar transformation is used. It rectifies the patch of image from Cartesian coordinates $[x, y]$ to polar coordinates $[d, \varphi]$ using the formula:

$$d = \sqrt{(x - x_0)^2 + (y - y_0)^2} \quad (3)$$

$$\varphi = \arctan(-\frac{y - y_0}{x - x_0}) \quad (4)$$

The center point, $[x_0, y_0]$, of the polar transformation is set to the center of the "eye". Figure 5 (c) shows the rectified marker of Figure 5 (b).

We label the connected components in the rectified image patch as did in the above section and compute the bounding rectangle of each labeled region. Then the angle of the black sector can be calculated by the ratio of width of bounding rectangle to that of image patch. The labeled regions that are on the ends of the patch must be merged before angle computation.

We can fill the code of each identified marker according to the position and angle of the black sector. A marker may correspond to multiple codes. So a look-up table which contains the code and its Identification Number is constructed beforehand. Through looking up the table, the marker is recognized.

5. Results

We have implemented our system in different environment and gotten the satisfactory results. Figure 6 (a) shows one experiment that a marker is put into a scene where some similar object exits, for example, the text on the book and the bar code on the plastic. Our system worked well in spite of these "noise".

Figure 6 (b) shows an experiment of a plane on which 32 markers are printed. The coordinate of the center of each marker is known. But the image of marker center is not the center of imagery elliptical "eye" center[14]. Both of them are very near if the image of the marker is small.

After camera calibration by using Heikkila's method[15], the toy on the plane is reconstructed. Figure 6 (d) shows the camera configuration and (c) shows the 3D model of the toy.

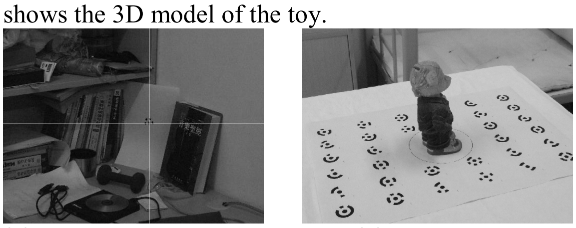

(a) Marker in a complex scene (b) Markers on plan

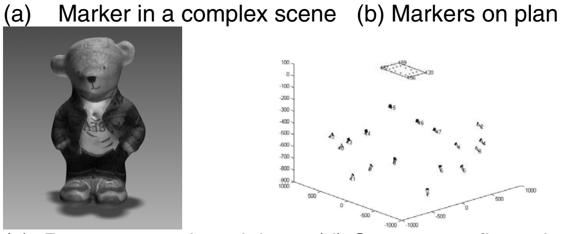

(c) Reconstructed model (d) Camera configuration

Figure 6. Experiment results

6. Conclusion

In this paper, we present a marker identification system. This system can be used in photogrammetry for automatic vision-based 3D measurement and also used in camera calibration without manual selection of matching points. We hope this system can be adapted to ubiquitous computing for object sensing in the future.

Acknowledgement

This project is supported by National Basic Research Program of China - 2006CB303105，Beijing Natural Science Foundation (No.4082025) and Doctoral Foundation of China (No.20070004037).

References

[1] Diego, L., et al., *TRIP: A Low-Cost Vision-Based Location System for Ubiquitous Computing.* Personal Ubiquitous Comput., 2002. **6**(3): p. 206-219.

[2] Naimark, L. and E. Foxlin. *Circular data matrix fiducial system and robust image processing for a wearable vision-inertial self-tracker*. in *Mixed and Augmented Reality,. Proceedings. International Symposium on*. 2002.

[3] Cho, Y., J. Lee, and U. Neumann. *A Multi-ring Color Fiducial System and an Intensity-invariant Detection Method for Scalable Fiducial-Tracking Augmented Reality* in *Proceedings of the 1st Intl. Workshop on Augmented Reality*. 1998. San Francisco.

[4] AhN, S.J., R. Wolfgang, and S.I. KIM, *Circular coded target for automation of optical 3D-measurement and camera calibration.* International journal of pattern recognition and artificial intelligence (Int. j. pattern recogn. artif. intell.), 2001. **15**(6): p. 905-919

[5] Claus, D. and A.W. Fitzgibbon, *Reliable Fiducial Detection in Natural Scenes*, in *Computer Vision - ECCV 2004*. 2004. p. 469-480.

[6] Fiala, M. *ARTag, a fiducial marker system using digital techniques*. in *Computer Vision and Pattern Recognition,. IEEE Computer Society Conference on, 2005*.

[7] PhotoModeler, http://www.photomodeler.com/.

[8] AICON, http://www.aicon.de/.

[9] 3DM-FotoMetrics, http://www.3dmedia.co.jp/.

[10] Jae, S.L., *Two-dimensional signal and image processing*. 1990: Prentice-Hall, Inc. 694 pages.

[11] Otsu, N., *A Threshold Selection Method from Gray-Level Histograms.* Systems, Man and Cybernetics, IEEE Transactions on, 1979. **9**(1): p. 62-66.

[12] Robert, S., *Algorithms in C.* 1990: Addison-Wesley Longman Publishing Co., Inc. 657 pages.

[13] Fitzgibbon, A., M. Pilu, and R.B. Fisher, *Direct least square fitting of ellipses.* Pattern Analysis and Machine Intelligence, IEEE Transactions on, 1999. **21**(5): p. 476-480.

[14] Joseph, L.M. and Z. Andrew, *Appendix-projective geometry for machine vision*, in *Geometric invariance in computer vision*. 1992, MIT Press. p. 463-519.

[15] Heikkila, J., *Geometric camera calibration using circular control points.* Pattern Analysis and Machine Intelligence, IEEE Transactions on, 2000. **22**(10): p. 1066-1077.